Neuro-Oncology Advance Access published January 17, 2013
Neuro-Oncology
doi:10.1093/neuonc/nos300
NEURO-ONCOLOGY

[^{18}F]-fluoro-ethyl-L-tyrosine PET: a valuable diagnostic tool in neuro-oncology, but not all that glitters is glioma

Markus Hutterer*, Martha Nowosielski*, Daniel Putzer, Nathalie L. Jansen, Marcel Seiz†, Michael Schocke, Mark McCoy, Georg Göbel, Christian la Fougère, Irene J. Virgolini, Eugen Trinka, Andreas H. Jacobs, and Günther Stockhammer

Department of Neurology (M.H., M.N., G.S.); Department of Nuclear Medicine (D.P., I.J.V.); Department of Radiology (M.S.); Department of Neurosurgery (M.S.†); Department of Medical Statistics, Informatics and Health Economics, Innsbruck Medical University, Austria (G.G.); Department of Neurology (M.H., E.T.); Division of Neuroradiology, Christian-Doppler Klinik, Paracelsus Medical University Salzburg, Austria (M.M.); Department of Neurology and Wilhelm-Sander Neurooncology Therapy Unit, University Hospital Regensburg, Regensburg, Germany (M.H.); Department of Nuclear Medicine, Munich Medical University, Campus Grosshadern, Munich, Germany (N.L.J., C.l.F.); European Institute for Molecular Imaging (EIMI) and Department of Nuclear Medicine, Westphalian Wilhelms University (WWU), Münster, Germany (A.H.J.); Department of Geriatric Medicine, Johanniter Krankenhaus, Bonn, Germany (A.H.J.)

Background. To assess the sensitivity and specificity of [^{18}F]-fluoro-ethyl-L-tyrosine (^{18}F-FET) PET in brain tumors and various non-neoplastic neurologic diseases.
Methods. We retrospectively evaluated ^{18}F-FET PET scans from 393 patients grouped into 6 disease categories according to histology ($n = 299$) or distinct MRI findings ($n = 94$) (low-grade/high-grade glial/nonglial brain tumors, inflammatory lesions, and other lesions). ^{18}F-FET PET was visually assessed as positive or negative. Maximum lesion-to-brain ratios (LBRs) were calculated and compared with MRI contrast enhancement (CE), which was graded visually on a 3-point scale (no/moderate/intense).
Results. Sensitivity and specificity for the detection of brain tumor were 87% and 68%, respectively. Significant differences in LBRs were detected between high-grade brain tumors (LBR, 2.04 ± 0.72) and low-grade brain tumors (LBR, 1.52 ± 0.70; $P < .001$), as well as among inflammatory (LBR, 1.66 ± 0.33; $P = .056$) and other brain lesions (LBR, 1.10 ± 0.37; $P < .001$). Gliomas ($n = 236$) showed ^{18}F-FET uptake in 80% of World Health Organization (WHO) grade I, 79% of grade II, 92% of grade III, and 100% of grade IV tumors. Low-grade oligodendrogliomas, WHO grade II, had significantly higher ^{18}F-FET uptakes than astrocytomas grades II and III ($P = .018$ and $P = .015$, respectively). ^{18}F-FET uptake showed a strong association with CE on MRI ($P < .001$) and was also positive in 52% of 157 nonglial brain tumors and nonneoplastic brain lesions.
Conclusions. ^{18}F-FET PET has a high sensitivity for the detection of high-grade brain tumors. Its specificity, however, is limited by passive tracer influx through a disrupted blood–brain barrier and ^{18}F-FET uptake in nonneoplastic brain lesions. Gliomas show specific tracer uptake in the absence of CE on MRI, which most likely reflects biologically active tumor.

Keywords: ^{18}F-FET PET, diagnostic value, glioma, MRI, brain tumor.

Received September 7, 2012; accepted October 19, 2012.

*These authors contributed equally as first authors.

Corresponding Author: Markus Hutterer, MD, Department of Neurology, Wilhelm-Sander Neurooncology Therapy Unit, University Hospital of Regensburg, Universitätsstraße 84, D-93053 Regensburg, Germany (markus.hutterer@kabelmail.de).

Magnetic resonance imaging (MRI) using T1, T2/fluid attenuated inversion recovery (FLAIR), and gadolinium-enhanced T1-weighted images is the standard neuroimaging method for brain tumor diagnosis. MRI provides excellent structural details with a high sensitivity but limited specificity, especially after previously applied radiation and/or chemotherapy.

Contrast-enhancing components on T1-weighted sequences (T1w) reflect blood–brain barrier (BBB) disruption and suggest a malignant tumor region. Signal abnormalities in T2/FLAIR-weighted images are a combination of nonenhancing tumor, perifocal edema, and treatment-related changes (gliosis, leukoencephalopathy, necrosis).[1]

Molecular imaging with positron emission tomography (PET) visualizing metabolic pathways has proven to overcome some of these limitations. Radiolabeled amino acids are of particular interest for brain tumor imaging because of their high uptake in biologically active tumor tissue but low uptake in normal brain tissue.[2] Within this group of radiopharmaceuticals, [^{18}F]-fluoro-ethyl-L-tyrosine (^{18}F-FET) is one of the most promising tracers.[3] In gliomas, ^{18}F-FET uptake significantly correlates with tumor cell density and proliferation rate as well as with microvascular density and neoangiogenesis, all biological hallmarks of highly malignant glial tumors.[4,5]

Several studies have clearly indicated that ^{18}F-FET PET—in combination with MRI—is able to improve the diagnostic and therapeutic assessment of patients with gliomas for neurosurgery[6–10] and radiotherapy planning.[11–19] Furthermore, ^{18}F-FET PET can be a valuable parameter to assess treatment response and predict survival in the course of radiotherapy, temozolomide chemotherapy, and anti-angiogenic treatment.[20,21]

Histological correlation studies with MRI and ^{18}F-FET PET have yielded a sensitivity of 93% and a specificity of 94% in glioma tissue.[6] Relatively small-sized patient cohorts with highly selected patient populations, however, limit the informative value of ^{18}F-FET PET in routine clinical neuro-oncology. Little is known about sensitivity and specificity of ^{18}F-FET PET in a large unselected patient population. Therefore, we retrospectively analyzed 393 ^{18}F-FET PET scans and compared them with the corresponding histopathological and MRI findings. First, we assessed sensitivity and specificity of ^{18}F-FET PET to identify a tumor-suspicious brain lesion on MRI as brain tumor. Secondly, we determined the maximum lesion-to-brain ratios (LBRs) for histologically verified gliomas in comparison with contrast enhancement (CE) on MRI T1w. Finally, for LBR and CE on MRI T1w from the total patient population, we defined and compared 6 disease categories: (i) low-grade glial brain tumors classified as World Health Organization (WHO) grades I–II, (ii) high-grade glial brain tumors WHO grades III–IV, (iii) low-grade nonglial brain tumors WHO grades I–II, (iv) high-grade nonglial brain tumors WHO grades III–IV, (v) inflammatory brain lesions, and (vi) other lesions.

Patients and Methods

Study Design

We retrospectively analyzed all ^{18}F-FET PET scans together with clinical and MRI data from patients who were examined at the Innsbruck Medical University Hospital between January 2004 and December 2010. All patients gave written informed consent before each ^{18}F-FET PET and MRI investigation as part of the clinical routine. In addition, this retrospective study was approved by the local ethics committee.

Inclusion criteria for further study analysis were (i) a clear diagnosis of a brain lesion (lesion histology and/or distinct MRI finding corresponding to clinical presentation) and (ii) an MRI performed by a standard protocol (T1 or T2 sequence, gadolinium-enhanced T1w) temporally corresponding with the ^{18}F-FET PET scan (range, $\pm$4 wk).

The study analysis resulted in 373 cases (Innsbruck patient cohort). The Innsbruck patient cohort was used for visual and LBR ^{18}F-FET PET analysis. In addition, 20 patients with nonglial brain tumors were enrolled from the Medical University of Munich (Munich patient cohort). Because of different PET devices and acquisition protocols, these cases were considered for only visual ^{18}F-FET PET analysis but not in further tracer uptake (ie, LBR) quantification.

Patient Population

The total study population consisted of 393 patients (228 male, 175 female) with a mean age of 44 years (range, 12–83 yr). According to histology ($n = 299$, 76%) or distinct MRI findings and clinical presentation ($n = 94$, 24%), the total patient cohort was grouped into the 6 disease categories we assigned, as noted.

The study population consisted of 236 (60%) glial tumors, 69 (18%) nonglial tumors, 13 (3%) active inflammatory brain lesions, and 74 (19%) other entities. Histology was available from all 236 (100%) glial brain tumors, 45/69 (65%) nonglial brain tumors, 8/13 (62%) inflammatory brain lesions, and 10/74 (14%) other entities. Patients without histological confirmation were included only if they showed characteristic MR findings with corresponding clinical presentation ($n = 94$, 24%).

The clinical indications for ^{18}F-FET PET studies were as follows: suspected brain tumor ($n = 154$, 39%), biopsy/surgery planning ($n = 74$, 19%), radiotherapy planning ($n = 12$, 3%), and response assessment following temozolomide ($n = 140$, 36%) or bevacizumab ($n = 13$, 3%) chemotherapy.

MRI Acquisition

All patients underwent MRI for routine neuroimaging diagnosis and/or treatment monitoring. MRI studies at the Medical University Hospital Innsbruck were conducted on a 1.5-Tesla scanner (Sonata, Siemens-Erlangen) and included a T1w 3-dimensional magnetization prepared rapid gradient echo (repetition time = 1860 ms, echo time = 4.38 ms with 1.2-mm slice thickness, 256 × 192 matrix), acquired pre- and postcontrast, as well as a T2w fast-spin echo sequence (6600 ms/100–110 ms, 2-mm slice thickness, 320 × 240 matrix). Postcontrast images were detected 5 min after

injection of contrast agent (Dotarem 0.1 mmol/kg, Omniscan).

MRI Analysis

For study analyses, all MRI scans were retrospectively reviewed by 2 independent experienced neuroradiologists blinded to histological diagnosis and ^{18}F-FET PET. During this review, CE on MRI T1w sequences was graded visually on a 3-point scale (no/moderate/intense CE).

^{18}F-FET PET Image Acquisition

^{18}F-FET PET acquisition was performed on 2 scanners. From January 2004 to December 2009, 271 18F-FET PET scans were conducted on a PET scanner (Advance, GE Healthcare) with a 15-cm axial field and a 28-cm transaxial field of view. The standard ^{18}F-FET dose was 150–180 MBq. ^{18}F-FET PET images were acquired in a 3D mode over 15 min from 35 contiguous transaxial slices of the entire brain with a slice thickness of 4.25 mm. Thirty minutes after intravenous tracer administration, the emission scan (15 min) was started. Thereafter, a transmission scan (5 min) was performed with a ^{67}germanium p-i-n source for attenuation correction. Reconstruction of the attenuation-corrected emission dataset was performed after filtered backprojection.

From January to December 2010, 102 ^{18}F-FET PET scans were conducted on a PET/CT scanner (GE Discovery PET/CT 690) using a transaxial reconstruction matrix of 256 × 256 (1 mm per pixel), acquiring 47 axial slices with a thickness of 3.27 mm. The standard ^{18}F-FET dose was 250 MBq. Thirty minutes after intravenous ^{18}F-FET application, the emission scan (5 min) was started. ^{18}F-FET PET images were acquired in a 3D mode in contiguous transaxial slices of the entire brain. Afterward, a low-dose CT was performed for attenuation correction purposes. An iterative reconstruction of the attenuation-corrected emission dataset was obtained using the ordered subset expectation maximization algorithm.

^{18}F-FET PET Image Analysis

^{18}F-FET PET image analysis was performed by an experienced nuclear medicine physician using Hermes Gold software 2.0. The visual assessment, determining whether an ^{18}F-FET PET scan was positive or negative, was done by an experienced nuclear physician in a 2-step process: first, image interpretation was done after software-based image fusion of ^{18}F-FET PET scans and corresponding MRIs. Since the physiologic background activity in ^{18}F-FET PET is very low, a second step compared ^{18}F-FET uptake in an MR-defined region with the background activity in the corresponding contralateral hemisphere, including white and gray matter. If the tracer uptake was higher compared with background activity, the lesion was considered positive. Visual image analysis was further used

Table 1. ^{18}F-FET PET uptake in brain tumors and other brain lesion subtypes

Brain Lesion Subtypes	Patients, *n* (%)[a]	Histology, *n* (%)[b]	^{18}F-FET Positive,[c] *n* (%)[b]	LBR,[d] median LBR ± SD
Brain tumors	305 (78)	281 (92)	261 (86)	1.87 ± 0.74
High grade				
WHO III–IV	169 (55)	161 (95)	160 (95)	2.04 ± 0.72
Low grade				
WHO I–II	136 (45)	120 (88)	101 (74)	1.52 ± 0.70
Glial brain tumors[e]	236 (60)	236 (100)	209 (89)	1.85 ± 0.74
High grade				
WHO III–IV	131 (56)	131 (100)	126 (96)	1.99 ± 0.74
Low grade				
WHO I–II	105 (44)	105 (100)	83 (79)	1.54 ± 0.69
Nonglial brain tumors[f]	70 (18)	47 (67)	53 (75)	1.95 ± 0.73
High grade				
WHO III–IV	39 (56)	31 (79)	35 (90)	2.09 ± 0.62
Low grade				
WHO I–II	31 (44)	16 (52)	18 (60)	1.38 ± 0.73
Inflammatory brain lesions[f]	13 (3)	8 (62)	13 (100)	1.66 ± 0.33
Other brain lesions[f]	74 (19)	10 (14)	16 (22)	1.10 ± 0.37
Total	393 (100)	299 (76)	291 (74)	1.65 ± 0.73

[a]Patient percents are related to total patient population ($N = 393$).
[b]Histology percents are related to brain lesion subtype.
[c]Visual ^{18}F-FET PET evaluation (total patient population, $N = 393$).
[d]^{18}F-FET uptake (LBR) quantification (Innsbruck patient population, $n = 373$).
[e]Refer to Table 2.
[f]Refer to Table 3.

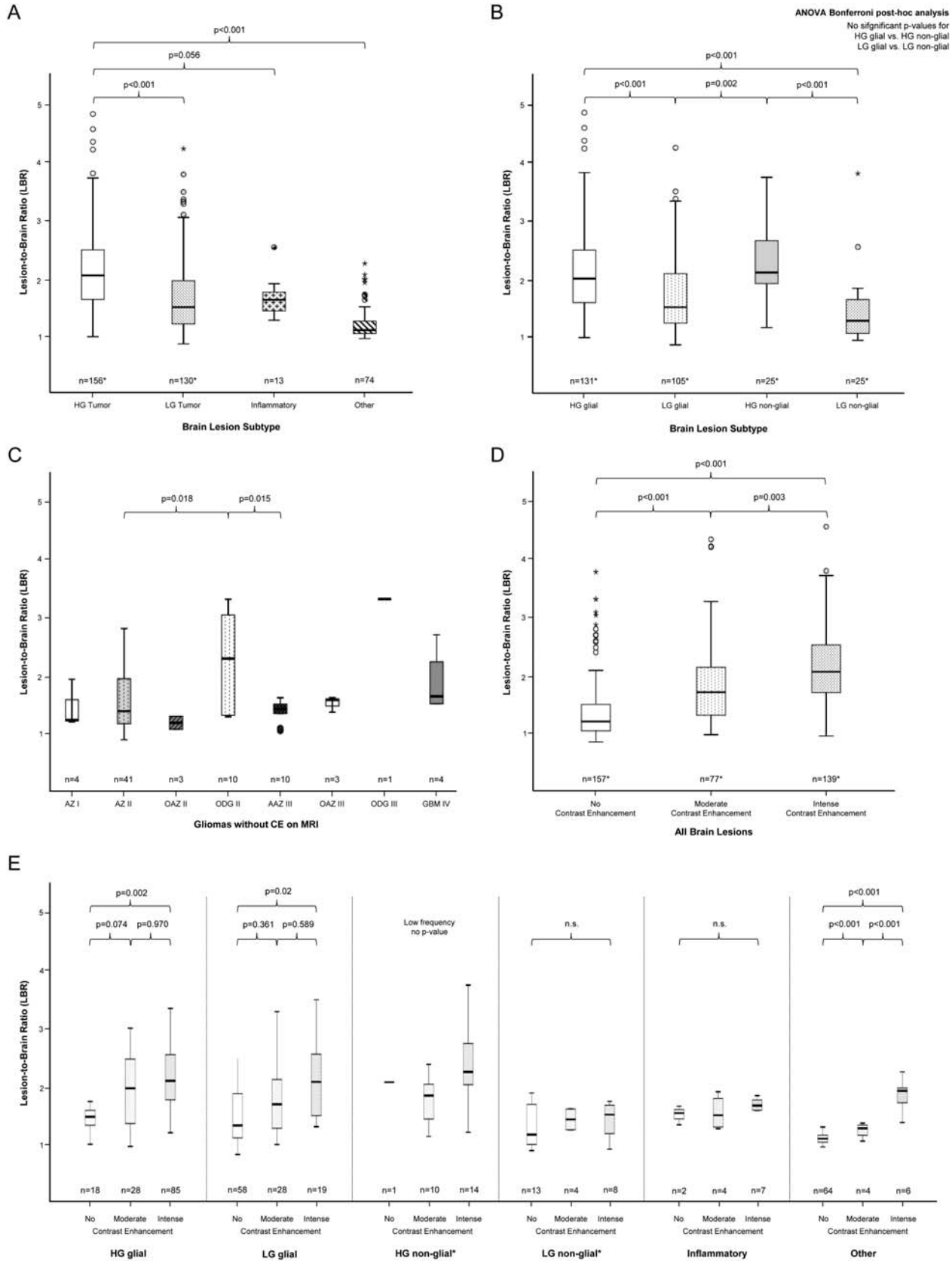

Fig. 1. Statistical analysis of LBR and CE on MRI T1w. (A) ^{18}F-FET uptake quantification (ie, LBR) according to histological subgroups and WHO grading. Significant differences in LBRs were detected between high-grade (HG) brain tumors (median LBR, 2.04 $\pm$ 0.72) and low-grade (LG) brain tumors (median LBR, 1.52 $\pm$ 0.70; $P < .001$), as well as among inflammatory brain lesions (median LBR, 1.66 $\pm$ 0.33; $P = .056$) and other

for the calculation of sensitivity, specificity, positive predictive value (PPV), and negative predictive value (NPV) to detect brain tumor.

To compare ^{18}F-FET uptake between different brain lesion subgroups, tracer uptake was quantified by means of standardized uptake values (SUVs) normalized to the patient's body weight using Rover Software (Advanced Biochemical Compounds). The regions of interest (ROIs) used for measuring the maximal activity of the entire brain lesion (SUV_{max}) were spheres with volumes covering the maximum diameters of the lesions. The size of the spherical ROIs was therefore different for each lesion. The ROI that was placed on the contralateral hemisphere (mirror region) to measure background activity was also spherical, and the volume range was 1.7 cm^3–2 cm^3, including white and gray matter. Afterward, the maximum LBRs were calculated and used for further statistical analysis.

Because of a PET device change in Innsbruck, we compared the LBRs of both scanners. No statistical difference in LBRs could be detected (*t*-test, $P = .787$).

Image Analysis at the University Hospital Munich

MRI and ^{18}F-FET PET scans at the University Hospital Munich were performed as described in previous studies.[22,23] The image analysis was retrospectively analyzed by an experienced nuclear physician and visually graded as positive or negative for brain tumor. Because of different PET devices and acquisition protocols, the patients from Munich were used for only visual ^{18}F-FET PET analysis (sensitivity/specificity calculation; Table 2) but were not considered for further tracer uptake (ie, LBR) quantification.

Statistics

Sensitivity and specificity were assessed by means of cross-table analysis using the data of visual ^{18}F-FET PET image analysis. An analysis of variance (ANOVA) and a correction for multiple comparisons (Bonferroni post-hoc analysis) were performed to evaluate differences among the histological subgroups and CE grading on MRI T1w. A 2-sided *t*-test was performed to compare differences between the 2 PET scanners. $P < .05$ was considered significant, with a confidence interval of 95%. Data were analyzed with SPSS 18.0 statistical software.

Results

^{18}F-FET Uptake in Brain Tumors Compared With Other Disease Categories

In the total patient population ($N = 393$), sensitivity and specificity for the detection of a brain tumor were 87% [95% CI: 84.5–91.3] and 68% [58.4–78.3], respectively; PPV and NPV were 91% [88.0–94.5] and 58% [48.6–68.8], respectively. When stratifying among WHO grades, ^{18}F-FET PET was able to identify 95% ($n = 161$) of high-grade and 88% ($n = 120$) of low-grade brain tumors. When discriminating between glial and nonglial brain tumor histology of all WHO grades, 89% ($n = 209$) of glial and 75% ($n = 52$) of nonglial brain neoplasms showed positive ^{18}F-FET uptake. ^{18}F-FET uptake was also detectable in 100% ($n = 13$) of inflammatory and 22% ($n = 16$) of other nonneoplastic brain lesions (Table 1), explaining the low specificity.

Comparison of LBR With Brain Lesion Categories

Six disease categories, defined from the Innsbruck patient population ($n = 373$ scans), were compared for LBRs. Significant differences in LBRs were detected between high-grade brain tumors ($n = 156$; median LBR, 2.04 ± 0.72) and low-grade brain tumors ($n = 130$; median LBR, 1.52 ± 0.70; $P < .001$), as well as among inflammatory ($n = 13$; median LBR, 1.66 ± 0.33; $P = .056$) and other brain lesions ($n = 74$; median LBR, 1.10 ± 0.37; $P < .001$) (Table 1, Fig. 1A). Importantly, there was no difference in median LBR when stratifying brain tumors according to glial and nonglial histology: high-grade glial ($n = 131$; median LBR, 1.99 ± 0.74) versus high-grade nonglial tumors ($n = 25$; median LBR, 2.09 ± 0.62) and low-grade glial ($n = 105$; median LBR, 1.54 ± 0.69) versus

brain lesions (median LBR, 1.10 ± 0.37; $P < .001$; ANOVA Bonferroni post-hoc analysis). (B) There was no LBR difference when stratifying the brain tumors to glial and nonglial histologies of HG glial (median LBR, 1.99 ± 0.74) vs HG nonglial tumor (median LBR, 2.09 ± 0.62) and LG glial (median LBR, 1.54 ± 0.69) vs LG nonglial tumor (median LBR, 1.38 ± 0.73). No significant differences were observed between HG gliomas and HG nonglial tumors or between LG gliomas and LG nonglial tumors. (C) Oligodendroglioma (ODG) WHO grade II (median LBR, 2.21 ± 0.88) showed significantly higher LBR than astrocytoma [A] grade II ($n = 41$, median LBR, 1.36 ± 0.19, $P = .018$) or anaplastic astrocytoma [AA] grade III ($n = 10$, median LBR, 1.55 ± 0.52, $P = .015$, ANOVA Bonferroni post-hoc analysis). No statistical difference was seen between glioblastoma (GBM) grade IV (median LBR, 1.86 ± 0.57) and oligoastrocytoma (OAZ) grade II (median LBR, 1.16 ± 0.16, $P = .091$) or between ODG II and A II. An ODG grade III ($n = 1$) showed the highest uptake of all brain lesions (LBR, 3.33). (D) Association between LBR and CE intensity on MRI (no CE, $n = 157$, median LBR = 1.42 ± 0.55; moderate CE, $n = 77$, median LBR = 1.88 ± 0.74; intense CE, $n = 139$, median LBR = 2.2 ± 0.67; $P < .001$, ANOVA Bonferroni post-hoc analysis). (E) CE intensity on MRI stratified to the 6 histological brain lesion subtypes. HG and LG brain tumors as well as inflammatory lesions showed positive tracer uptake despite absence of CE. In the "other" group, ^{18}F-FET signal intensity is directly associated with CE on MRI. *LBR calculation: only patients from the Innsbruck patient cohort ($n = 373$) were considered; PA, pilocytic astrocytoma, astrocytoma, oligodendroglioma; OA, oligoastrocytoma; AA, anaplastic astrocytoma; AOA, anaplastic oligoastrocytoma; AO, anaplastic oligodendroglioma; GBM, glioblastoma.

Table 2. ^{18}F-FET uptake dependent on CE intensity on MRI T1w in gliomas

Histological Subtype, WHO Grade[b]	Total CE[a]		No CE[a]		Moderate CE[a]		Intense CE[a]	
	Patients, *n*	^{18}F-FET Positive, *n* (%)[c]	Patients, *n* (%)[d]	^{18}F-FET Positive, *n* (%)[c]	Patients, *n* (%)[d]	^{18}F-FET Positive, *n* (%)[c]	Patients, *n* (%)[d]	^{18}F-FET Positive, *n* (%)[c]
Pilocytic astrocytoma								
WHO I	10	8 (80)	4 (40)	2 (50)	2 (20)	2 (100)	4 (40)	4 (100)
Glioma								
WHO II	95	75 (79)	54 (57)	37 (69)	26 (27)	23 (88)	15 (16)	15 (100)
Astrocytoma	70	53 (76)	41 (59)	26 (63)	16 (23)	14 (100)	13 (18)	13 (100)
Oligoastrocytoma	7	5 (71)	3 (43)	1 (33)	4 (57)	4 (100)	–	–
Oligodendroglioma	18	17 (94)	10 (56)	10 (100)	6 (33)	5 (83)	2 (11)	2 (100)
Anaplastic glioma								
WHO III	63	58 (92)	14 (22)	12 (86)	18 (29)	15 (83)	31 (49)	31 (100)
Astrocytoma	46	41 (89)	10 (22)	8 (80)	15 (32)	12 (80)	21 (46)	21 (100)
Oligoastrocytoma	7	7 (100)	3 (43)	3 (100)	–	–	4 (57)	4 (100)
Oligodendroglioma	10	10 (100)	1 (10)	1 (100)	3 (30)	3 (100)	6 (60)	6 (100)
Glioblastoma								
WHO IV	68	68 (100)	4 (6)	4 (100)	10 (15)	10 (100)	54 (79)	54 (100)
Total								
WHO I–IV	236	209 (89)	76 (32)	55 (72)	56 (24)	50 (89)	104 (44)	104 (100)

[a]CE = contrast enhancement on MRI T1w.
[b]Low-grade glial tumor = WHO I–II; high-grade glial tumor = WHO III–IV.
[c]Patient percents are related to the CE subgroup.
[d]Patient percents are related to the histological subtype.

low-grade nonglial tumor ($n = 25$; median LBR, 1.38 ± 0.73) (Table 1, Fig. 1B). When stratifying to glial/nonglial histology and tumor grading, ^{18}F-FET PET was able to distinguish between high-grade versus low-grade glial ($P < .001$) and high-grade versus low-grade nonglial brain tumors ($P < .001$) (Fig. 1B).

^{18}F-FET Uptake in Gliomas

Table 2 gives an overview of ^{18}F-FET uptake in histologically confirmed glioma WHO grades I–IV ($n = 236$) and its association with CE intensity on MRI T1w. Remarkably, 100% ($n = 68$) of glioblastoma grade IV, 92% ($n = 58$) of anaplastic glioma grade III, 79% ($n = 75$) of glioma grade II, and 80% ($n = 8$) of pilocytic astrocytoma grade I presented with positive ^{18}F-FET uptake in visual PET analysis.

Evaluation of CE-negative gliomas, defined as a glial brain tumor subgroup with characteristic T2 hyperintensity but without CE on MRI T1w, showed that ^{18}F-FET occurs in 50% ($n = 2$) of pilocytic glioma WHO grade I, 69% ($n = 37$) of glioma grade II, 86% ($n = 12$) of anaplastic glioma grade III, and 100% ($n = 4$) of glioblastoma grade IV (Table 2), indicating a specific tracer uptake in biologically active brain tumor tissue. Further analysis of this subgroup (excluding unspecific ^{18}F-FET uptake secondary to an enhanced BBB permeability) revealed that oligodendroglioma grade II ($n = 10$; median LBR, 2.21 ± 0.88) presented with a significantly higher LBR than astrocytoma grade II ($n = 41$; median LBR, 1.36 ± 0.19, $P = .018$) or astrocytoma grade III ($n = 10$; median LBR, 1.55 ± 0.52, $P = .015$, ANOVA Bonferroni post-hoc analysis; Fig. 1C). Remarkably, in this large patient population, 1 oligodendroglioma grade III showed the highest ^{18}F-FET uptake (LBR, 3.33) of all analyzed brain lesions.

Comparison of CE on T1w MRI With Disease Categories

The ^{18}F-FET LBR showed a strong dependency with CE on MRI T1w, graded visually on a 3-point scale (no CE, $n = 157$, median LBR = 1.42 ± 0.55; moderate CE, $n = 77$, median LBR = 1.88 ± 0.74; intense CE, $n = 139$, median LBR = 2.2 ± 0.67; $P < .001$, ANOVA Bonferroni post-hoc analysis; Fig. 1D). Comparison of LBR and CE according to the 6 brain lesion subtypes revealed similar significant associations within each subtype (Fig. 1E).

^{18}F-FET Uptake in Nonglial Brain Tumors and Other Brain Lesions

As detailed in Table 3, ^{18}F-FET uptake was frequently observed in several non-astroglial/non-oligodendroglial primary brain tumors WHO grades I–IV (eg, ependymoma, primitive neuroectodermal tumor, primary CNS lymphoma), metastases of various solid primaries (eg, adenocarcinomas of lung and breast, melanoma), extra-axial brain tumors (eg, meningioma, acoustic neurinoma), active inflammatory (eg, multiple sclerosis/acute disseminated encephalomyelitis plaques, bacterial

Table 3. [18]F-FET uptake in various nonglial brain lesions

Brain Lesion Subtypes	Patients, *n*	Histology, *n* (%)	[18]F-FET Positive, *n* (%)[a]
Total	157[b]	65 (41)	82 (52)
Nonglial high-grade brain tumors			
WHO III–IV	39	31 (79)	35 (90)
Embryonic tumors			
Medulloblastoma			
WHO IV	4	4 (100)	2 (50)
Pinealoblastoma			
WHO IV	2	2 (100)	2 (100)
Primitive neuroectodermal tumor			
WHO IV	3	3 (100)	3 (100)
Primary CNS lymphoma			
WHO IV	6	6 (100)	6 (100)
EBV-associated lymphoproliferation			
WHO IV	1	1 (100)	1 (100)
Reticulosarcoma (skull base)			
WHO IV	1	1 (100)	1 (100)
Ependymoma			
WHO III	6	6 (100)	5 (83)
Meningioma			
WHO III	2	2 (100)	2 (100)
Cerebral metastases[c]			
Mamma carcinoma	5	3 (60)	5 (100)
Bronchus tumor (adenocarcinoma)	3	–	3 (100)
Bronchus tumor (small cell lung cancer)	1	–	1 (100)
Melanoma	3	2 (67)	3 (100)
Ovarial carcinoma	1	–	1 (100)
Reticulosarcoma	1	1 (100)	–
Nonglial low-grade brain tumors			
WHO I–II	31	16 (52)	18 (60)
Ependymoma			
WHO II	3	3 (100)	3 (100)
Meningioma			
WHO II	5	1 (20)	4 (80)
Dysembryoplastic neuroepithelial tumor			
WHO I	9	2 (22)	2 (22)
Gangliocytoma			
WHO I	1	1 (100)	1 (100)
Ganglioglioma			
WHO I	3	3 (100)	2 (67)
Papillary glioneural tumor			
WHO I	1	1 (100)	–
Hemangioblastoma			
WHO I	1	1 (100)	1 (100)
Neurinoma (*N. acusticus*)			
WHO I	2	1 (50)	2 (100)
Neurofibroma (neurofibromatosis type I)			
WHO I	1	–	1 (100)
Schwannoma			
WHO I	1	–	1 (100)
Craniopharyngioma			
WHO I	1	1 (100)	1 (100)
Pituitary gland adenoma			
WHO I	2	1 (100)	–
Dermoid cyst (mature teratoma)			
WHO I	1	1 (100)	–
Inflammatory brain lesions (active)	13	8 (62)	13 (100)
MS plaques	7	2 (29)	7 (100)
ADEM lesions	1	1 (100)	1 (100)
Progressive multifocal leukoencephalopathy	1	1 (100)	1 (100)
Isolated CNS vasculitis	1	1 (100)	1 (100)
Limbic encephalitis	1	1 (100)	1 (100)
Mastoiditis	1	1 (100)	1 (100)
Meningoencephalitis secondary to mastoiditis	1	1 (100)	1 (100)
Other brain lesions	74	10 (14)	16 (22)
Malformations			
Cortical dysplasia[d]	22	1 (5)	7 (32)
Cavernoma	8	1 (14)	5 (63)
Hamartoma	7	–	–
Neuroepithelial cysts	3	–	–
Gliosis			
Post-inflammatory: ADEM/MS and rare cases[e]	17	3 (25)	–
Post-ischemic: chronic vascular and poststroke	10	3 (50)	–
Leukoencephalopathy (mitochondropathy)	1	1 (100)	–
Hippocampus sclerosis	3	1 (33)	1 (33)
Subacute brain lesions			
Cerebral contusion area (subacute phase)	1	–	1 (100)
Ischemic lesion (subacute phase)	2	–	2 (100)

Abbreviations: EBV, Epstein–Barr virus; MS, multiple sclerosis; ADEM, acute disseminated encephalomyelitis.
[a]Visual [18]F-FET PET evaluation.
[b]The patient population of $n = 157$ consists of 137 patients from Innsbruck and 20 patients from Munich.
[c]Multiple cerebral metastases were counted as one.
[d]Cortical dysplasia, localization in MRI, *n* (%): temporal 6 (28), corpus amygdaloideum 6 (28), frontal 4 (19), hippocampus 2 (10), gyrus cinguli 1 (5), insula 1 (5), cerebellar 1 (5).
[e]Neurosarcoidosis, status postherpes encephalitis.

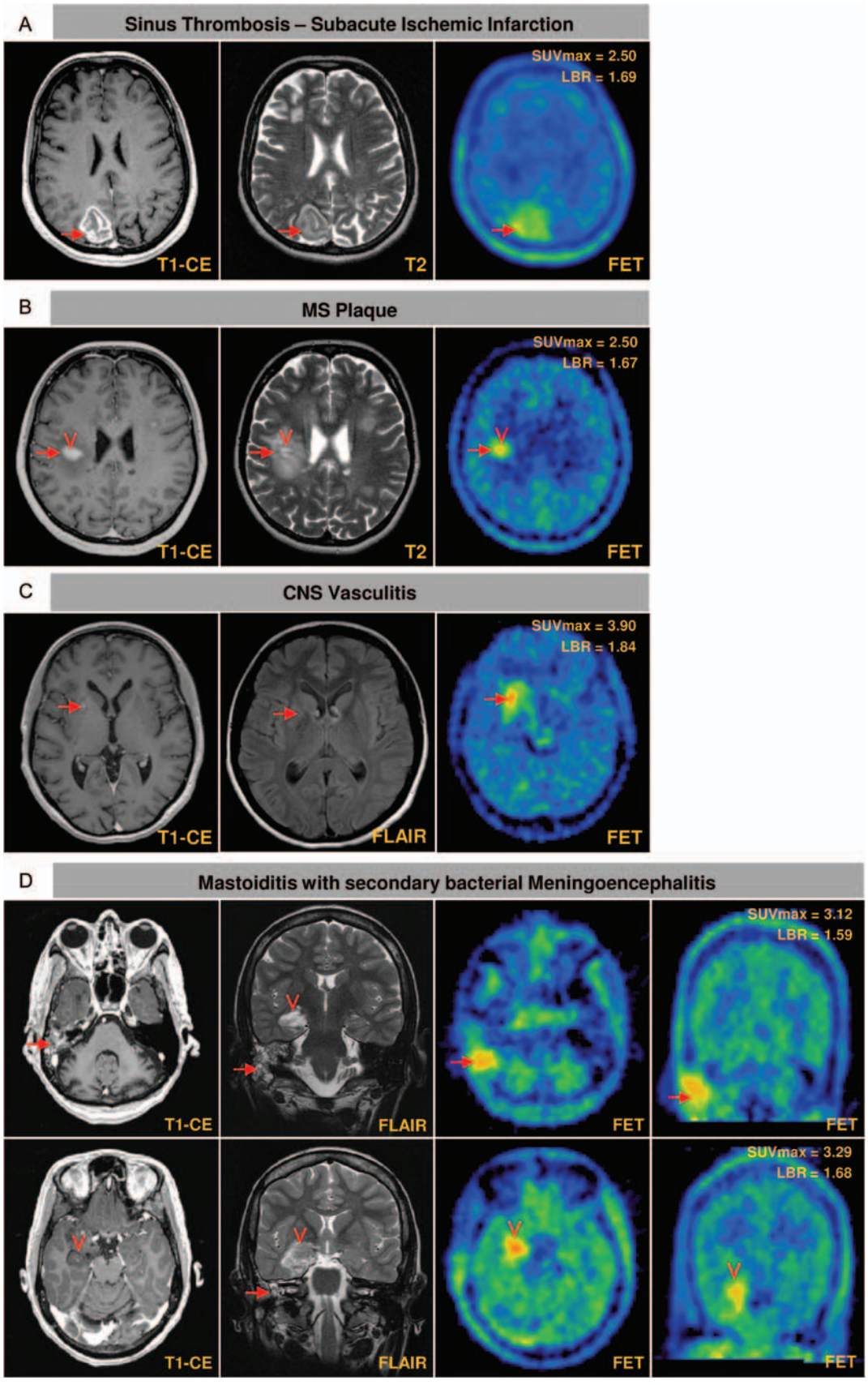

meningoencephalitis, progressive multifocal leukencephalopathy) and other brain lesions (eg, vascular and cerebral malformations, including cavernoma and cortical dysplasia).

Significant ^{18}F-FET uptake was also observed in subacute ischemic (Fig. 2A; Supplementary material, Fig. S1) and traumatic brain lesions, which were associated with CE on MRI T1w. ^{18}F-FET uptake was also detected in several active inflammatory brain lesions with CE (eg, multiple sclerosis plaque; Fig. 2B) and without CE (eg, CNS vasculitis [Fig. 2C], bacterial meningoencephalitis [Fig. 2D]) on MRI T1w. This observation indicates that ^{18}F-FET uptake may also occur in active inflammatory brain lesions independently of an enhanced BBB permeability. Importantly, LBRs of inflammatory lesions (median LBR, 1.66 ± 0.33) were similar to those of low-grade brain tumors (median LBR, 1.52 ± 0.70) and significantly lower than in high-grade brain tumors (median LBR, 1.99 ± 0.74) (Table 1). In contrast, inactive T2 signal hyperintensities (glioses) of various underlying pathologies (chronic-vascular, post-ischemic, post-inflammatory, posttraumatic, post-surgery; Table 3) showed no ^{18}F-FET uptake.

Discussion

At present, limited experience derived from small-sized patient cohorts of highly selected patient populations has posed the question of the benefit of ^{18}F-FET PET for routine clinical neuro-oncologic practice. Therefore, we performed a retrospective study of a large unselected patient population, including various neoplastic and non-neoplastic neurologic diseases, investigating the diagnostic value of ^{18}F-FET PET in addition to routine MRI. The results of this study show that ^{18}F-FET PET has a high sensitivity for the detection of brain tumor, irrespective of whether the tumor is of glial or nonglial origin. The specificity of ^{18}F-FET PET detecting brain tumors as a single modality is low, limited by passive tracer influx through disrupted BBB and tracer uptake in nonneoplastic brain lesions. Gliomas, however, show specific tracer uptake irrespective of BBB disruption.

The finding that ^{18}F-FET PET has a high sensitivity (87%) for the detection of brain tumors is in line with a recently published meta-analysis. In a series including 462 patients from 13 studies, Dunet et al.[24] investigated the value of ^{18}F-FET PET to identify newly diagnosed tumor-suspicious brain lesions as brain tumors versus nontumor lesions and found a pooled sensitivity of 82% for detecting brain tumors. Despite the difference in the numbers of glial versus nonglial tumors included, similar results can be explained by our finding that most brain tumors are positive irrespective of whether the tumor is of glial or nonglial origin.

In our patient cohort, the specificity of ^{18}F-FET detecting brain tumors was low (68%), which can be explained by ^{18}F-FET tracer uptake in several non-neoplastic brain lesions. So far, the literature contains only case reports and case series describing ^{18}F-FET uptake in nonglial lesions,[25–29] including inflammatory brain lesions,[3,26,27,30,31] acute and subacute ischemic infarctions,[27,32] and intracranial hemorrhage,[6,33] which are partially included in the meta-analysis by Dunet et al.[24] Therefore, primary brain tumor diagnosis can certainly be done only by histological confirmation.

The diagnostic accuracy of ^{18}F-FET PET to detect brain tumors may be improved in combination with additional molecular MR-based methods. For example, Floeth et al.[3] analyzed the diagnostic value of ^{18}F-FET PET in combination with MR spectroscopy in patients with newly diagnosed glioma-suspicious brain lesions on MRI ($N = 50$). For PET as a single method, sensitivity and specificity of ^{18}F-FET uptake for the distinction of neoplastic and non-neoplastic lesions were 88% and 88%, respectively. The sensitivity for the preoperative identification of gliomas using MR alone was 68% and could be increased to 97% when MRI was combined with ^{18}F-FET PET and MR spectroscopy.

Within the various disease categories of our study, LBR calculation proved to be a useful tool to discriminate between high-grade and low-grade brain tumors, as well as among inflammatory and other brain lesions. ^{18}F-FET uptake with LBRs of ≥ 2.0 could be attributed to biologically active tumor tissue of a high-grade brain tumor. LBR calculation, however, was not able to differentiate brain tumors of glial versus nonglial origins.

Low-grade brain tumors, with the exception of oligodendrogliomas, presented with LBRs of ~ 1.5, which is in the range of inflammatory and other active (eg, ischemic, traumatic) brain lesions but clearly higher than for nonactive residual gliotic lesions. These findings indicate that low ^{18}F-FET uptake is not tumor specific.

A subanalysis of low-grade gliomas confirmed recently reported findings that low-grade oligodendrogliomas have significantly increased LBRs compared with other low-grade tumors,[34] which may even be higher than uptake in high-grade astrocytomas WHO grades III–IV. This elevated tracer uptake has been ascribed to the increased cellular and vascular density in this glioma subtype.[35]

Fig. 2. ^{18}F-FET uptake in subacute ischemic and active inflammatory brain lesions. (A) Patient with a subacute ischemic infarction after a venous sinus thrombosis with CE on MRI T1w due to enhanced BBB permeability within the infarct area. The BBB disruption causes unspecific tracer uptake by passive non-carrier-mediated influx into the brain parenchyma. (B) A patient with multiple sclerosis presented with a subcortical active inflammatory brain lesion with central CE. Patients with active neuroinflammatory brain lesions, (C) primary CNS vasculitis, (D) mastoiditis of the right ear with secondary bacterial meningoencephalitis. Both active inflammatory brain lesions showed an intensive focal ^{18}F-FET uptake independently of CE on MRI T1w.

^{18}F-FET tracer accumulation was strongly associated with CE on MRI T1w independently of brain lesion histology, reflecting a passive tracer influx due to enhanced BBB permeability. In this context, an important finding was that 72% of 76 low-grade and high-grade glial brain tumors lacking CE on MRI showed ^{18}F-FET uptake. Therefore, tracer uptake unrelated to unspecific tracer influx does exist, which is in line with the results of a recently published study on ^{18}F-FET PET in non-CE brain lesions suspicious for low-grade gliomas.[36] This observation also supports the concept of an active ^{18}F-FET uptake mechanism into tumor and vascular cells of biologically active tumor tissue.[4,5] Similar results were recently also shown for combined [^{11}C]-methionine PET/MRI, which was able to better delineate the true extent of metabolically active tumor tissue in nonenhancing anaplastic gliomas compared with MRI alone.[37] In addition, the use of ^{18}F-FET PET in combination with MRI has already proven valuable in clinical practice. A focally enhanced ^{18}F-FET uptake identifying the most malignant part of a tumor independently of CE on MRI was demonstrated to be useful for optimized biopsy site planning.[6,22,30,38] ^{18}F-FET PET has also been shown to better determine biological tumor volume and the tumor infiltration border zone than does MRI alone. This information may, in future, aid to improve tumor resection[6,26,30] and radiotherapy target-volume planning.[15,39] In addition, Galldiks et al.[20] recently showed that ^{18}F-FET PET can be used to better assess treatment response in glioblastoma after first-line therapy and predict survival compared to MRI alone.

Finally, it has to be mentioned that to a limited extent, increased ^{18}F-FET uptake was also found in acute inflammatory brain lesions independently of BBB permeability, with LBRs up to 1.5. In animal experiments, less tracer uptake into inflammatory lesions was observed with ^{18}F-FET compared with ^{18}F-fluorodeoxyglucose, postulating that this amino acid tracer may therefore show higher tumor specificity.[40,41] Our study and case series, however, have revealed that active inflammatory brain lesions in humans may also show ^{18}F-FET uptake with LBRs comparable to those of low-grade brain tumors.[3,26,27,30,31,42] The exact mechanism of ^{18}F-FET uptake in inflammatory processes, other than through a disrupted BBB, is currently unknown.

Conclusion

This is the first study of a large unselected patient population demonstrating that (i) ^{18}F-FET PET has a high sensitivity for the detection of brain tumors and (ii) ^{18}F-FET PET, based on LBR calculation, is able to differentiate between high-grade and low-grade brain tumors, irrespective of glial or nonglial histology. The interpretation of ^{18}F-FET uptake in the LBR range of 1.5–2.0 is limited due to nonspecific tracer uptake into areas with enhanced BBB permeability and inflammation. Therefore, primary brain tumor diagnosis can certainly be done only by histological confirmation. Importantly, ^{18}F-FET PET positive glial brain tumors without CE on MRI confirm a specific tracer uptake into biologically active tumor tissue independently of BBB breakdown.

Supplementary Material

Supplementary material is available at *Neuro-Oncology Journal* online (http://neuro-oncology.oxfordjournals.org/).

Acknowledgments

This study was presented in part in abstract form at the 2010 ASCO meeting in Chicago, IL and the 2011 SNO meeting in Orange County, CA. We disclose editorial consideration in another journal and in previous reports or publications.

Conflict of interest statement. All authors have seen and agreed with the contents of the manuscript. The authors have no conflicts of interest related to this work and confirm the originality of this study.

Funding

M. H. holds a grant from the Oesterreichische Nationalbank Jubiläumsfond (project number 14326). M. N. holds a DOC-fFORTE Fellowship from the Austrian Academy of Science. All authors were independent of the funders in all aspects of study design, data analysis, and writing of the manuscript.

References

1. Jain R, Scarpace LM, Ellika S, et al. Imaging response criteria for recurrent gliomas treated with bevacizumab: role of diffusion weighted imaging as an imaging biomarker. *J Neurooncol*. 2010;96(3):423–431.
2. Jager PL, Vaalburg W, Pruim J, de Vries EG, Langen KJ, Piers DA. Radiolabeled amino acids: basic aspects and clinical applications in oncology. *J Nucl Med*. 2001;42(3):432–445.
3. Floeth FW, Pauleit D, Wittsack HJ, et al. Multimodal metabolic imaging of cerebral gliomas: positron emission tomography with [18F]fluoroethyl-L-tyrosine and magnetic resonance spectroscopy. *J Neurosurg*. 2005;102(2):318–327.
4. Stockhammer F, Plotkin M, Amthauer H, van Landeghem FK, Woiciechowsky C. Correlation of F-18-fluoro-ethyl-tyrosin uptake with vascular and cell density in non-contrast-enhancing gliomas. *J Neurooncol*. 2008;88(2):205–210.

5. Ullrich R, Backes H, Li H, et al. Glioma proliferation as assessed by 3′-fluoro-3′-deoxy-L-thymidine positron emission tomography in patients with newly diagnosed high-grade glioma. *Clin Cancer Res*. 2008;14(7):2049–2055.
6. Pauleit D, Floeth F, Hamacher K, et al. O-(2-[18F]fluoroethyl)-L-tyrosine PET combined with MRI improves the diagnostic assessment of cerebral gliomas. *Brain*. 2005;128(Pt 3):678–687.
7. Tanaka Y, Nariai T, Momose T, et al. Glioma surgery using a multimodal navigation system with integrated metabolic images. *J Neurosurg*. 2009;110(1):163–172.
8. Plotkin M, Blechschmidt C, Auf G, et al. Comparison of F-18 FET-PET with F-18 FDG-PET for biopsy planning of non-contrast-enhancing gliomas. *Eur Radiol*. 2010;20(10):2496–2502.
9. Floeth FW, Stummer W. The value of metabolic imaging in diagnosis and resection of cerebral gliomas. *Nat Clin Pract Neurol*. 2005;1(2):62–63.
10. Floeth FW, Sabel M, Ewelt C, et al. Comparison of (18)F-FET PET and 5-ALA fluorescence in cerebral gliomas. *Eur J Nucl Med Mol Imaging*. 2011;38(4):731–741.
11. Grosu AL, Weber WA. PET for radiation treatment planning of brain tumours. *Radiother Oncol*. 2010;96(3):325–327.
12. Grosu AL, Weber WA, Franz M, et al. Reirradiation of recurrent high-grade gliomas using amino acid PET (SPECT)/CT/MRI image fusion to determine gross tumor volume for stereotactic fractionated radiotherapy. *Int J Radiat Oncol Biol Phys*. 2005;63(2):511–519.
13. Piroth MD, Holy R, Pinkawa M, et al. Prognostic impact of postoperative, pre-irradiation (18)F-fluoroethyl-l-tyrosine uptake in glioblastoma patients treated with radiochemotherapy. *Radiother Oncol*. 2011;99(2):218–224.
14. Piroth MD, Pinkawa M, Holy R, et al. Integrated-boost IMRT or 3-D-CRT using FET-PET based auto-contoured target volume delineation for glioblastoma multiforme—a dosimetric comparison. *Radiat Oncol*. 2009;4:57.
15. Weber DC, Zilli T, Buchegger F, et al. [(18)F]Fluoroethyltyrosine- positron emission tomography-guided radiotherapy for high-grade glioma. *Radiat Oncol*. 2008;3:44.
16. Weber DC, Casanova N, Zilli T, et al. Recurrence pattern after [(18)F]fluoroethyltyrosine-positron emission tomography-guided radiotherapy for high-grade glioma: a prospective study. *Radiother Oncol*. 2009;93(3):586–592.
17. Rickhey M, Moravek Z, Eilles C, Koelbl O, Bogner L. 18F-FET-PET-based dose painting by numbers with protons. *Strahlenther Onkol*. 2010;186(6):320–326.
18. Rickhey M, Koelbl O, Eilles C, Bogner L. A biologically adapted dose-escalation approach, demonstrated for 18F-FET-PET in brain tumors. *Strahlenther Onkol*. 2008;184(10):536–542.
19. Niyazi M, Geisler J, Siefert A, et al. FET-PET for malignant glioma treatment planning. *Radiother Oncol*. 2011;99(1):44–48.
20. Galldiks N, Langen KJ, Holy R, et al. Assessment of treatment response in patients with glioblastoma using O-(2-18F-fluoroethyl)-L-tyrosine PET in comparison to MRI. *J Nucl Med*. 2012;53(7):1048–1057.
21. Hutterer M, Nowosielski M, Putzer D, et al. O-(2-18F-fluoroethyl)-L-tyrosine PET predicts failure of antiangiogenic treatment in patients with recurrent high-grade glioma. *J Nucl Med*. 2011;52(6):856–864.
22. Kunz M, Thon N, Eigenbrod S, et al. Hot spots in dynamic (18)FET-PET delineate malignant tumor parts within suspected WHO grade II gliomas. *Neuro Oncol*. 2011;13(3):307–316.
23. Popperl G, Kreth FW, Mehrkens JH, et al. FET PET for the evaluation of untreated gliomas: correlation of FET uptake and uptake kinetics with tumour grading. *Eur J Nucl Med Mol Imaging*. 2007;34(12):1933–1942.
24. Dunet V, Rossier C, Buck A, Stupp R, Prior JO. Performance of 18F-fluoro-ethyl-tyrosine (18F-FET) PET for the differential diagnosis of primary brain tumor: a systematic review and metaanalysis. *J Nucl Med*. 2012;53(2):207–214.
25. Pauleit D, Stoffels G, Schaden W, et al. PET with O-(2-18F-fluoroethyl)-L-tyrosine in peripheral tumors: first clinical results. *J Nucl Med*. 2005;46(3):411–416.
26. Pauleit D, Stoffels G, Bachofner A, et al. Comparison of (18)F-FET and (18)F-FDG PET in brain tumors. *Nucl Med Biol*. 2009;36(7):779–787.
27. Pichler R, Dunzinger A, Wurm G, et al. Is there a place for FET PET in the initial evaluation of brain lesions with unknown significance? *Eur J Nucl Med Mol Imaging*. 2010;37(8):1521–1528.
28. Kasper BS, Struffert T, Kasper EM, et al. 18Fluoroethyl-L-tyrosine-PET in long-term epilepsy associated glioneuronal tumors. *Epilepsia*. 2011;52(1):35–44.
29. Weckesser M, Langen KJ, Rickert CH, et al. O-(2-[18F]fluorethyl)-L-tyrosine PET in the clinical evaluation of primary brain tumours. *Eur J Nucl Med Mol Imaging*. 2005;32(4):422–429.
30. Floeth FW, Pauleit D, Sabel M, et al. 18F-FET PET differentiation of ring-enhancing brain lesions. *J Nucl Med*. 2006;47(5):776–782.
31. Pichler R, Wurm G, Nussbaumer K, Kalev O, Silye R, Weis S. Sarcoidosis and radiation-induced astrogliosis causes pitfalls in neuro-oncologic positron emission tomography imaging by O-(2-[18F]fluoroethyl)-L-tyrosine. *J Clin Oncol*. 2010;28(36):e753–e755.
32. Jacobs A. Amino acid uptake in ischemically compromised brain tissue. *Stroke*. 1995;26(10):1859–1866.
33. Mehrkens JH, Popperl G, Rachinger W, et al. The positive predictive value of O-(2-[18F]fluoroethyl)-L-tyrosine (FET) PET in the diagnosis of a glioma recurrence after multimodal treatment. *J Neurooncol*. 2008;88(1):27–35.
34. Giammarile F, Cinotti LE, Jouvet A, et al. High and low grade oligodendrogliomas (ODG): correlation of amino-acid and glucose uptakes using PET and histological classifications. *J Neurooncol*. 2004;68(3):263–274.
35. Fortin D, Cairncross GJ, Hammond RR. Oligodendroglioma: an appraisal of recent data pertaining to diagnosis and treatment. *Neurosurgery*. 1999;45(6):1279–1291.
36. Jansen NL, Graute V, Armbruster L, et al. MRI-suspected low-grade glioma: is there a need to perform dynamic FET PET? *Eur J Nucl Med Mol Imaging*. 2012;39(6):1021–1029.
37. Galldiks N, Kracht LW, Dunkl V, et al. Imaging of non- or very subtle contrast-enhancing malignant gliomas with [(11)C]-methionine positron emission tomography. *Mol Imaging*. 2011;10(6):453–459.
38. Floeth FW, Sabel M, Stoffels G, et al. Prognostic value of 18F-fluoroethyl-L-tyrosine PET and MRI in small nonspecific incidental brain lesions. *J Nucl Med*. 2008;49(5):730–737.
39. Niyazi M, Geisler J, Siefert A, et al. FET-PET for malignant glioma treatment planning. *Radiother Oncol*. 2011;99(1):44–48.
40. Kaim AH, Weber B, Kurrer MO, et al. (18)F-FDG and (18)F-FET uptake in experimental soft tissue infection. *Eur J Nucl Med Mol Imaging*. 2002;29(5):648–654.
41. Rau FC, Weber WA, Wester HJ, et al. O-(2-[(18)F]Fluoroethyl)-L-tyrosine (FET): a tracer for differentiation of tumour from inflammation in murine lymph nodes. *Eur J Nucl Med Mol Imaging*. 2002;29(8):1039–1046.
42. Pauleit D, Floeth F, Tellmann L, et al. Comparison of O-(2-18F-fluoroethyl)-L-tyrosine PET and 3-123I-iodo-alpha-methyl-L-tyrosine SPECT in brain tumors. *J Nucl Med*. 2004;45(3):374–381.